

RESEARCH

Open Access



Zinc oxide nanoparticle regulates the ferroptosis, proliferation, invasion and steamiess of cervical cancer by miR-506-3p/CD164 signaling

Jie-Yun Lei¹, Shuang-Xue Li², Feng Li³, Hui Li^{4*} and Yuan-Sheng Lei^{5*}

*Correspondence:
708927510@qq.com;
leiyuanshenglife@163.com

¹The University of Sheffield,
Sheffield, England

²Department of Respiratory
Medicine, People's Hospital
Affiliated to Shanxi Medical
University, Taiyuan, Shanxi, China

³Department of General Surgery,
Taigang General Hospital
Affiliated to Shanxi Medical
University, Taiyuan, Shanxi, China

⁴Department of Gynecology,
People's Hospital Affiliated
to Shanxi Medical University,
Taiyuan, Shanxi, China

⁵Department of Neurology, The
Second Affiliated Clinical Medical
College of Shanxi Medical
University, Taiyuan, Shanxi, China

Abstract

Background: Cancer stem cell (CSC) and ferroptosis play critical roles in cancer development, but the underlying mechanisms remain unclear. Cervical cancer induces a great mortality and an increased incidence globally. Zinc oxide nanoparticle is the nanomaterial that has been applied in industrial products and targets multiple cancer cell types and cancer stem cells. Here, we aimed to explore the effect of ZON on CSC and ferroptosis of cervical cancer.

Methods: In the present study, we identified that the treatment of ZON in vitro inhibited the proliferation of cervical cancer cells.

Results: The ZON stimulated the apoptosis of cervical cancer cells. The tumor growth of cervical cancer cells was attenuated by ZON in the xenograft mouse model in vivo. Meanwhile, ZON represses cell invasion and migration of cervical cancer. Crucially, the sphere formation numbers were repressed by ZON. Meanwhile, the SP ratio of cervical cancer cells was inhibited by ZON. The expression of CSC markers, including Sox-2, Oct3/4, and Nanog, was suppressed by circFoxo3 inhibition. Moreover, the ferroptosis was enhanced by ZON in cervical cancer cells. About the mechanism, we observed that ZON enhanced miR-506-3p expression and CD164 was a target of miR-506-3p, in which ZON inhibited CD164 expression by promoting miR-506-3p in cervical cancer cells. We validated that CD164 reversed miR-506-3p-mediated stemness and ferroptosis in cervical cancer cells. ZON repressed stemness and reduced ferroptosis of cervical cancer cells by targeting CD164. ZON inhibits cell growth of cervical cancer in vivo by targeting CD164.

Conclusions: In brief, we concluded that ZON regulated the ferroptosis, proliferation, invasion, and steamiess of cervical cancer by miR-506-3p/CD164 signaling. Our finding provides new insights into the mechanism by which ZON regulates ferroptosis and steamiess of cervical cancer by a miR-506-3p/CD164 axis.

Keywords: Cervical cancer, Cancer stem cell, Ferroptosis, ZON, miR-506-3p, CD164



Background

Cervical cancer is one of the common female malignancy and is the leading cause of mortality in women (Cohen et al. 2019). Cervical cancer is a leading cause of cancer death of women and the distribution of cervical cancer varies widely, with >85% of the global burden occurring in low-income and middle-income countries (Cohen et al. 2019). Over the last decades, trends in cervical cancer incidence and mortality have been observed to vary in different countries (Cohen et al. 2019). Most patients with cervical cancer receive radiotherapy and adjuvant chemotherapy, which can significantly improve patient survival, but excessive chemoresistance, radioresistance, and metastasis limit the effectiveness of the treatment (Bhatla and Singhal 2020; Vu et al. 2018; The 2020). Therefore, exploring novel treatments for cervical cancer is significant and important. Over the past two decades, the concept of cancer stem cell (CSC) has notably improved the understanding of cancer progression. CSCs are a small portion of cancer cells that exhibit self-renewal and differentiation abilities (Lytle et al. 2018). Targeting stemness could be a feasible approach for cervical cancer therapy. Besides, recent studies revealed that ferroptosis, a special form of cell death induced by iron-dependent lipid peroxidation, play a critical role in cancer development (Yagoda et al. 2007; Alvarez et al. 2017; Liu et al. 2020; Hu et al. 2020). For instance, ferroptosis participated in drug resistance during cancer therapy (Wang et al. 2021), and ferroptosis-related gene signature was proposed as a predictive biomarker for tumor progression (Liu et al. 2020; Mou et al. 2019). Moreover, Zinc oxide nanoparticle (Song et al. 2017) is the nanomaterial that has been applied in industrial products and is capable of targeting multiple cancer cell types and cancer stem cells (Steele et al. 2009; Hu and Du 2020).

MiR-506-3p was reported as a tumor suppressor in several cancers by targeting the 3'UTR region of oncogenes. For instance, miR-506-3p suppresses YAP1 expression and the subsequent tumorigenesis of thyroid cancer (Chen et al. 2020). Shang et al. suggested that miR-506-3p suppresses cell proliferation and metastasis of colorectal cancer via targeting the transforming growth factor- β 1 (TGF- β 1) (Shang et al. 2020). CD164 is a type I integral transmembrane glycoprotein that belongs to sialomucin family (Forde et al. 2007). CD164 was primarily identified as a surface marker of CD34+ human hematopoietic progenitor cells, as well as regulating its proliferation, adhesion, and differentiation (Doyonnas et al. 2000). Besides, CD164 expression is correlated with muscle regeneration and various biological processes during cancer progression (Bae et al. 2008). For example, CD164 is capable of regulating bone metastasis of cancer cells (Havens et al. 2006). Tang and colleagues found that the knockdown of CD164 could suppress the proliferation and mobility of colon cancer cells (Tang et al. 2012). Therefore, CD164 is regarded as a potential diagnostic biomarker and therapeutic target for cancer therapy.

In this research, we aimed to investigate the function of ZON treatment in the regulation of ferroptosis and stemness of cervical cancer, and identified decreased proliferation, metastasis, stemness, and enhanced ferroptosis of cervical cancer cells by ZON. Mechanistically, ZON blocked miR-506-3p/CD164 regulatory axis, leading to inhibited expression of CD164.

Materials and methods

Materials

sh-CD164, scramble control sequence (sh-NC), miR-506-3p mimics and inhibitor, and CD164 (pcDNA-CD164), were brought from RiboBio Co., Ltd. (China). EGF, bFGF, B27, methylcellulose, and ferroptosis inducer Erastin was obtained from Sigma-Aldrich (Zhou et al. 2019). Antibodies for ABCG2, C-Myc, Bmi1, Sox2, Vimentin, E-cadherin, CD164, and β -Catenin were purchased from Proteintech (China).

Cells lines and treatment

Human cervical cancer cell lines Hela (CCL-2, ATCC, USA) and C33A (HTB-31, ATCC, USA), and normal cervical epithelial cells HcerEpic (AC340374, ATCC, USA) were obtained from American Type Culture Collection (ATCC, USA) was cultured in DMEM (Gibco, USA) containing 10% FBS (Gibco, USA) at 37 °C incubator with 5% CO₂. To activate ferroptosis, cells were treated with Erastin at a dose of 5 μ g/ml for 8 h after indicated cell transfection.

The Synthesis and Characterization of ZON

ZON were synthesized by refluxing the precursor zinc acetate dihydrate (0.1 M) in ethane-1,2-diol and triglycol at 180 °C and 220 °C, respectively. The time of the reaction was for 2–3 h in the presence of sodium acetate (0.01 M). The solution was put on a magnetic stirrer at 80 °C for 1.5 h and centrifuged at 8000 rpm for 15 min and rinsed with deionized water and ethyl alcohol 3 times. Finally, the samples were dried at 80 °C overnight. ZON dose was dissolved in deionized water till the complete dissolution. Size, morphology, and elemental composition were observed and measured by a transmission electron microscope (TEM, JEOL, Japan), while the surface zeta potential measurements were also measured by a zeta potential analyzer (Malvern Device, UK) (Nabil et al. 2020).

Cell counting kit 8 (CCK-8)

Cell viability was detected using CCK-8 kit (Thermo). Hela and C33A cells were digested and seeded in 96-well plate. After seeding for 0, 24, 48, 72, and 96 h, CCK-8 reagent was added into each well to incubate for another 1 h. Then, the optical density (OD) at 450 nm was detected by a microplate reader (BioTech, USA).

Colony formation assay

Hela and C33A cells were digested and seeded in 6-well plate (1000 cells per well), and cultured for 2 weeks. The visible colonies were fixed with methanol, followed by staining with 0.2% crystal violet for twelve minutes, and were captured by a digital camera.

Cell apoptosis

Hela and C33A cells were transfected with sh-circFoxo3, and/or circFoxo3 overexpressing vector for 48 h, digested, and collected for detection of apoptosis using a

Annecin-V/PI Apoptosis Detection Kit (Thermo) in accordance with manufacturer's description.

Cell migration and invasion

Cell migration was determined by Transwell and wound healing experiment. For Transwell assay, cells were suspended in FBS-free medium and seeded in top chambers, and the lower chambers contained complete medium. After incubation for 24 h, the cells migrated to the lower side of top chambers were stained with 0.2% crystal violet and captured. For wound healing experiment, cell monolayer was scratched by a 200 μ l pipette, washed with PBS, and cultured in FBS-free media. The migration ability was evaluated by calculating cell movement into the scratched area drawn at 0–24 h.

Sphere formation

Hela and C33A cells were subjected to indicated treatment, digested and seeded in 96-well ultra-low-attachment plates (Corning) at a density of 500 cells per well for 10 days. The culture medium consists of DMEM/F12 medium (Hyclone), 10 ng/mL EGF, 20 ng/mL bFGF, B27 (1:50), and 20% methylcellulose. The spheres were photographed by microscope (Leica, Germany).

Western blotting

Western blotting assay was performed following a standard procedure. In short, total protein was extracted from Hela and C33A cells after treatment, separated in sodium dodecyl sulfate polyacrylamide gel electrophoresis (SDS–PAGE), shifted to NC membranes. Then, the membranes were soaked in blocking solution (Sigma-Aldrich) for 15 min, incubated with indicated primary antibodies at 4 °C for one night, and subsequently hatched with corresponding secondary antibodies at room temperature for 45 min. The protein bands were then reacted with enhanced chemiluminescent solution (ECL, Millipore, USA).

Quantitative real-time PCR (qRT-PCR)

For quantification of miR-506-3p and CD164, total RNA was extracted by Trizol reagent and reverse-transcribed using a cDNA reverse transcription kit (Thermo). For miR-506-3p quantification, the RNA was subjected to an All-in-One™ miRNA cDNA Synthesis Kit (GeneCopoeia, USA). qRT-PCR was conducted using a SYBR kit (Thermo). The relative expression were calculated using the $2^{-\Delta\Delta CT}$ method. The CD164 expression was normalized by GAPDH. The miR-506-3p expression was normalized by U6 small nuclear RNA. The primers were as following:

miR-506-3p, sense 5'-ACACTCATAAGGCACCCTTC-3',
antisense 5'-TCTACTCAGAAGGGGAGTAC-3';
CD164, sense 5'-ACCCGAACGTGACGACTTTAG-3',
antisense 5'-CGTGTCCCCACTTGACAATC-3';
GAPDH, sense 5'-CTTTGGTA TCGTGGAAGGACTC-3',
antisense 5'-GTAGAGGCAGGGATGATGTTCT-3';
U6, sense 5'-GCTTCGGCAGCACATATACTAAAA T-3',
antisense 5'-CGCTTCACGAA TTTGCGTGTCA T-3'.

Identification of ferroptosis

To identify the occurrence of ferroptosis, we detected the levels of glutathione (GSH), malondialdehyde (MDA), ROS and intracellular iron using GSH assay kit (Beyotime, China), MDA assay kit (Beyotime), C11-BODIPY (Beyotime), and Iron Assay Kit (Beyotime) following the manufacturer's protocols.

Dual luciferase reporter gene assay

Recombinant vectors of pMIR-CD164 wild-type (WT), pMIR-CD164 mutant (MUT), were synthesized by RiboBio (China). HeLa and C33A cells were transfected by WT or MUT luciferase reporter vectors along with miR-506-3p mimics for 24 h. Activity of luciferase was measured using dual luciferase reporter assay system (Promega) in accordance with manufacturer's description.

Mice xenograft model

6-week aged BALB/C nude mice were ordered from Vital River Laboratory (China) and randomly divided into three groups. C33A and HeLa cells (5×10^6) were planted into the right flank of mice. Tumor size ($(\text{length} \times \text{width}^2)/2$) and mice body weight were measured every 5 days for 30 days. The mice were then sacrificed and tumors were collected for immunohistochemical (IHC) analysis and western blotting experiment. This study was carried out in accordance with the recommendations in the Guide for the Care and Use of Laboratory Animals of the National Institutes of Health. The protocol was approved by the Committee on the Ethics of Animal Experiments of Shanxi Provincial People's Hospital.

IHC staining

Tumor tissue were fixed in 4% polyformaldehyde (PFA), embedded with paraffin, and sliced into 4- μm sections. Subsequently, the tissue slides went through dewaxing, rehydration, antigen repair, blocking, incubation with antibody against Ki67 (Proteintech) and HRP-conjugated secondary antibody (Proteintech). The labelled sections were then stained by DAB solution and hematoxylin (Beyotime). The positive staining was photographed by microscope (Leica) and calculated by Image J.

Statistical analysis

All results were presented as the mean \pm standard deviation (SD), and analyzed using an SPSS 20.0 software. The statistical differences between two or multiple groups were calculated by Student's *t* tests or one-way analysis of variance (ANOVA) followed by Tukey's post hoc test. The *p* values lower than 0.05 was considered as statistically significant.

Results

ZON suppresses cell growth of cervical cancer

The ZON was synthesized and the actual size and surface charge were observed by TEM and zeta potential analyzer. The average particle size = 38 nm, the zeta potential

of ZON was -20 mV, zeta deviation = 3.0 mV, and conductivity = 0.1 mS/cm (Additional file 1: Fig. S1).

Hela and C33A cells were digested and seeded in 6-well plate (1000 cells per well), and cultured for 2 weeks. Functionally, the colony formation assays showed that the colony numbers of Hela and C33A cells, but not normal cervical epithelial cells HcerEpic, were repressed by the treatment of ZON (Fig. 1A and Additional file 1: Fig. S2A). The flow cytometry assay revealed that the treatment of ZON stimulated the apoptosis of Hela and C33A cells (Fig. 1B). Importantly, the tumor growth of C33A cells was attenuated by treatment of ZON in the xenograft mouse model in vivo (Fig. 1C, E).

ZON represses cell invasion and migration of cervical cancer

To evaluate the function of ZON on invasion and migration of cervical cancer cells, transwell assays were performed. We found that the invasion and migration of Hela and C33A cells were suppressed by ZON (Fig. 2A, B). Meanwhile, wound healing assays showed that the wound closure was inhibited by ZON in Hela and C33A cells (Fig. 2C, D). In addition, ZON up-regulated E-cadherin expression and down-regulated Vimentin expression at mRNA and protein levels (Fig. 2E, F).

ZON attenuates stemness of cervical cancer cells

CSCs properties play crucial roles in cancer development, and then we were interested in the effect of ZON on stemness of cervical cancer cells. The sphere formation

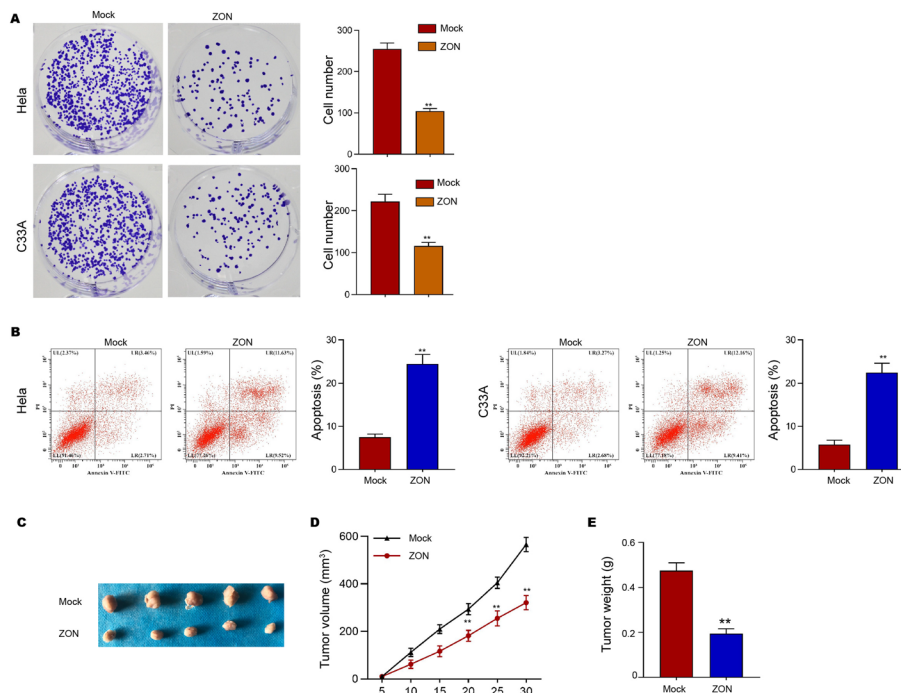


Fig. 1 ZON suppresses cell growth of cervical cancer. **A, B** Cervical cancer cells were treated with ZON. **A** Hela and C33A cells were digested and seeded in 6-well plate (1000 cells per well), and cultured for 2 weeks. The cell growth was analyzed by colony formation assays. **B** Cell apoptosis was tested by flow cytometry analysis. **C–E** Tumor growth of C33A cell was analyzed by xenograft mouse model in vivo ($n = 5$). Mock, equal volume of deionized water. The experiments were repeated 3 times, $**P < 0.01$

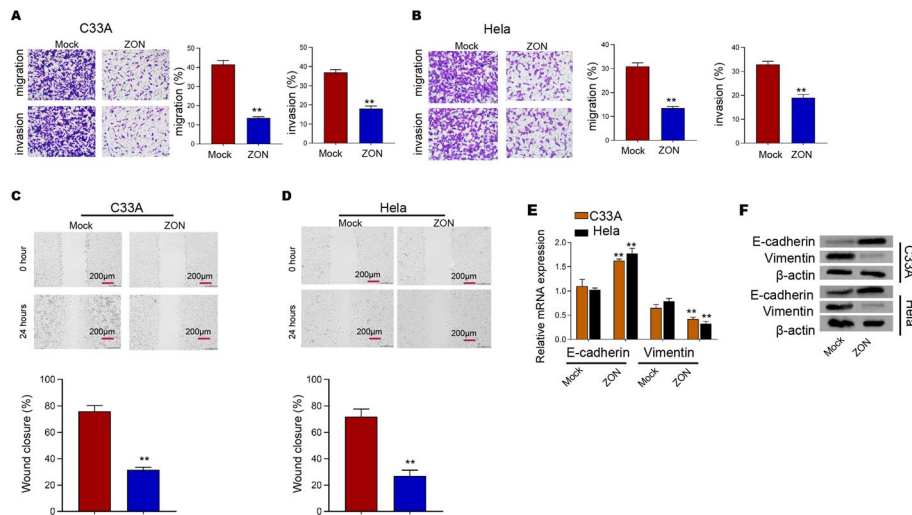


Fig. 2 ZON represses cell invasion and migration of cervical cancer. **A–F** Cervical cancer cells were treated with ZON. **A, B** Cell invasion and migration were analyzed by transwell assays. **C, D** Cell migration was detected by wound healing assays. **E** mRNA of E-cadherin and Vimentin was validated by qPCR. **F** Protein levels of E-cadherin and Vimentin were detected by Western blot. The experiments were repeated 3 times, ** $P < 0.01$

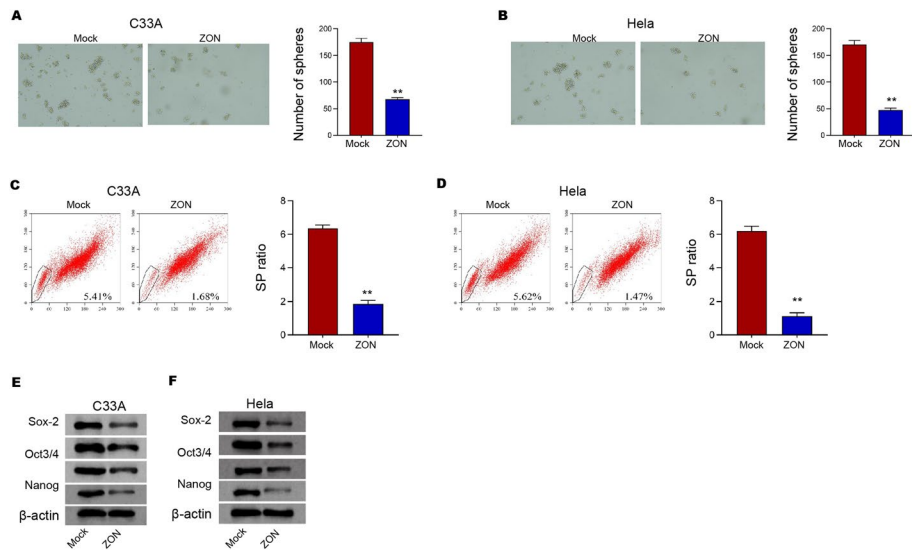


Fig. 3 ZON attenuates stemness of cervical cancer cells. **A–F** Cervical cancer cells were treated with ZON. **A, B** Sphere formation efficiency was detected by sphere formation assays. **C, D** Hoechst 33,342 staining-positive cells was analyzed by flow cytometry analysis in the cells. **E, F** Expression of Sox-2, Oct3/4, and Nanog was measured by Western blot. The experiments were repeated 3 times, ** $P < 0.01$

numbers were repressed by ZON in HeLa and C33A cells (Fig. 3A, B). Meanwhile, the flow cytometry assay revealed that the SP ratio of HeLa and C33A cells was inhibited by ZON (Fig. 3C, D). In addition, the expression of CSC markers, including Sox-2, Oct3/4, and Nanog, was suppressed by ZON in HeLa and C33A cells (Fig. 3E, F).

ZON induces ferroptosis of cervical cancer cells

Given that ferroptosis is a critical phenotype of cancer progression, we further assessed whether ZON affected ferroptosis of cervical cancer cells. We observed that the treatment of ZON significantly repressed HeLa and C33A cell viabilities and ferroptosis inhibitor Ferrostatin rescued the viabilities in the cells (Fig. 4A). Moreover, the levels of GSH were inhibited by ZON but Ferrostatin rescued the phenotype in HeLa and C33A cells (Fig. 4B, C). Consistently, the levels of MDA, lipid ROS, and iron were induced by ZON in HeLa and C33A cells, while Ferrostatin reversed the ZON-stimulated induction (Fig. 4D, I).

ZON represses CD164 by enhancing miR-506-3p

Interestingly, we observed that ZON enhanced the expression of miR-506-3p in HeLa and C33A cells (Fig. 5A). The binding site between miR-506-3p and CD164, a critical factor in cancer development (Fig. 5B). The luciferase activity of CD164 was decreased by miR-506-3p in HeLa and C33A cells (Fig. 5C). MiR-506-3p mimic inhibited CD164 expression in HeLa and C33A cells (Fig. 5D). Significantly, the expression of CD164 was repressed by ZON in HeLa and C33A cells, in which the suppression of miR-506-3p by its inhibitor reversed this repression (Fig. 5E).

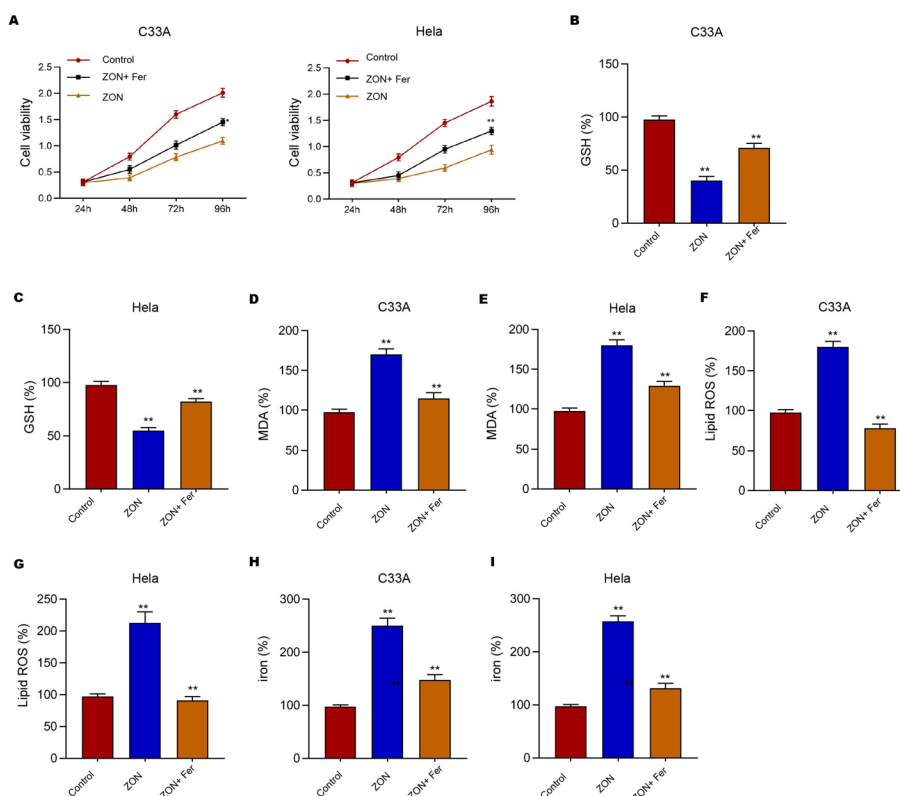


Fig. 4 ZON induces ferroptosis of cervical cancer cells. **A** Cell viability was detected by CCK-8 assays. **C–I** Levels of GSH (**B, C**), MDA (**D, E**), lipid ROS (**F, G**), and iron (**H, I**) were analyzed. The experiments were repeated 3 times, ** $P < 0.01$

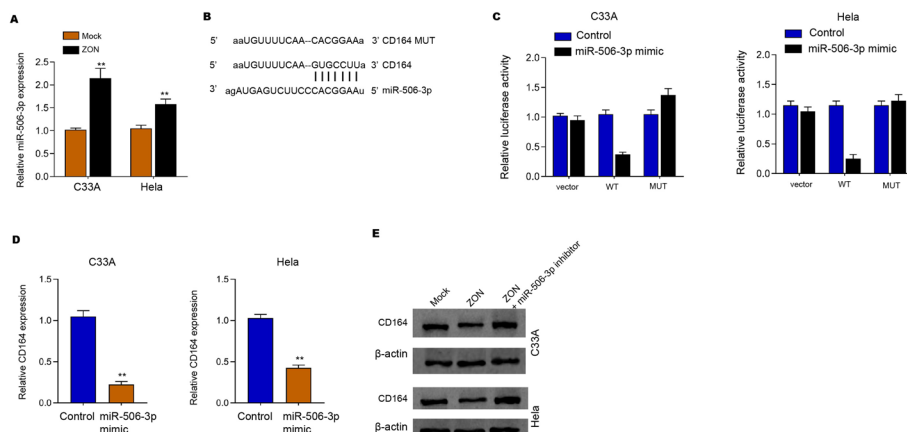


Fig. 5 ZON represses CD164 by enhancing miR-506-3p. **A** Expression of miR-506-3p was measured by qPCR in cervical cancer cells treated with ZON. **B** Wild type and mutant binding sites of CD164 with miR-506-3p. **C, D** Cervical cancer cells were treated with miR-506-3p mimic. **C** Luciferase activity of CD164 was detected by dual luciferase reporter gene assays. **D** Expression of CD164 was analyzed by qPCR. **E** Expression of CD164 was determined by Western blot in the cervical cancer cells. The experiments were repeated 3 times, ***P* < 0.01

CD164 reverses miR-506-3p-mediated stemness and ferroptosis of cervical cancer cells

Next, we further verified the correlation of CD164 and miR-506-3p in the regulation of stemness and ferroptosis of cervical cancer cells. We found that the treatment of miR-506-3p mimic repressed sphere formation numbers of HeLa and C33A cells and CD164 overexpression rescued this phenotype in the cells (Fig. 6A, B). The GSH level were increased but the MDA, lipid ROS, and iron levels were decreased by miR-506-3p inhibitor in RSL3 stimulated HeLa and C33A cells, while CD164 silencing by shRNA could reversed the effect of miR-506-3p inhibitor in the cells (Fig. 6C, J).

ZON represses stemness and reduces ferroptosis of cervical cancer cells by targeting CD164

Furthermore, we then further validated the correlation of ZON and CD164 in the regulation of stemness and ferroptosis of cervical cancer cells. We found that the treatment of ZON inhibited sphere formation numbers of HeLa and C33A cells and CD164 overexpression rescued this phenotype in the cells (Fig. 7A, B). The GSH level were reduced but the MDA, lipid ROS, and iron levels were enhanced by ZON in HeLa and C33A cells, while CD164 overexpression reversed the effect of ZON but miR-506-3p could reverse the effect of CD164 in the cells (Fig. 7C, J).

Meanwhile, we validated that the tumor growth of C33A and HeLa cells was repressed by ZON in the xenograft mouse model in vivo, in which the overexpression of CD164 could reverse the effect of ZON (Fig. 8A, B, Additional file 1: Fig. S3A and B). In addition, the levels of Ki-67 and CD164 were validated in the model (Fig. 8C, D, Additional file 1: Fig. S3C and D).

Discussion

Cervical cancer is a prevalent female malignancy with high aggressiveness and increasing incidence globally. In this research, we discovered the crucial roles of ZON in the regulation of proliferation, ferroptosis, invasion, and CSCs of cervical cancer cells.

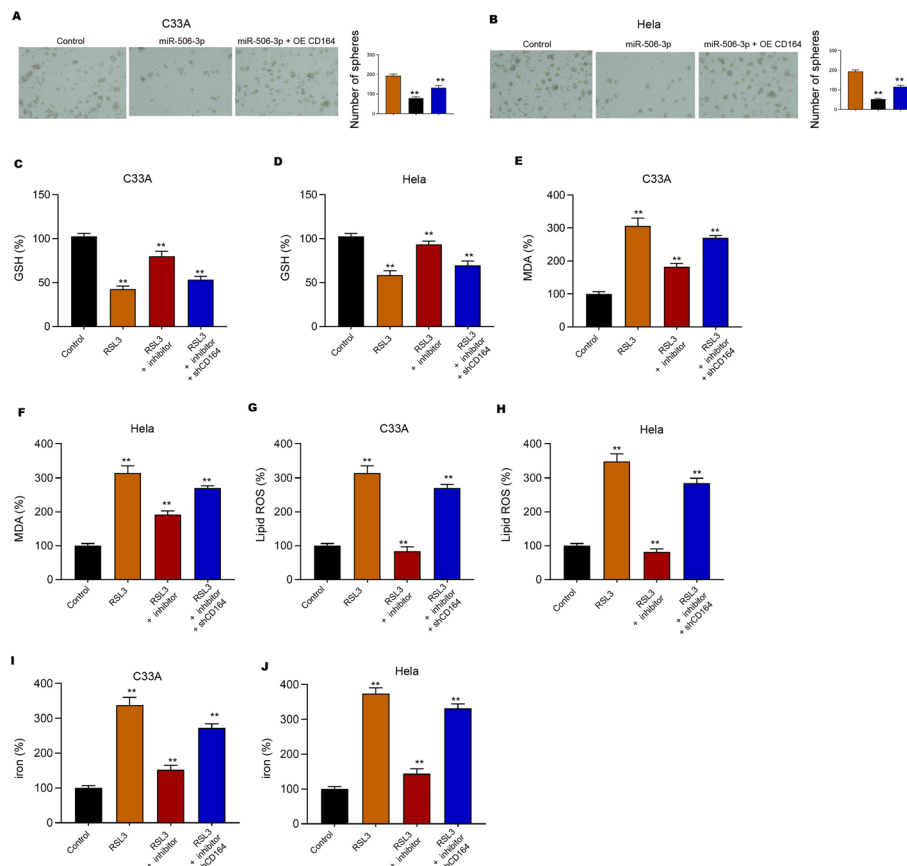


Fig. 6 CD164 reverses miR-506-3p-mediated stemness and ferroptosis of cervical cancer cells. **A, B** Cervical cancer cells were treated with miR-506-3p mimic or co-treated with CD164 overexpressing vectors. The sphere formation efficiency was detected by sphere formation assays. **C–J** RSL3 (1 μ M)-stimulated cervical cancer cells were treated with miR-506-3p inhibitor or co-treated with miR-506-3p inhibitor and CD164 shRNA. The levels of GSH (**C, D**), MDA (**E, F**), lipid ROS (**G, H**), and iron (**I, J**) were analyzed. The experiments were repeated 3 times, ** $P < 0.01$

Previous investigations indicate the anti-tumor effect of ZON in cancer development. It has been found that ZON induces apoptosis and oxidative stress in cancer cells (Wahab et al. 2014). Chitosan-capped ZON regulates apoptosis and cell cycle arrest by inducing p53 in cancer cells (Anitha et al. 2019). Frizzled-7-targeted delivery of ZON modulates drug resistance of cancer cells (Ruenraroengsak et al. 2019). Our data uncovered that the treatment of ZON in vitro inhibited the proliferation of cervical cancer cells. The ZON stimulated the apoptosis of cervical cancer cells. ZON attenuated the tumor growth of cervical cancer cells in the xenograft mouse model in vivo. Meanwhile, ZON represses cell invasion and migration of cervical cancer. Crucially, the sphere formation numbers were repressed by ZON. Meanwhile, the SP ratio of cervical cancer cells was inhibited by ZON. The expression of CSC markers, including Sox-2, Oct3/4, and Nanog, was suppressed by circFoxo3 inhibition. Moreover, the ferroptosis was enhanced by ZON in cervical cancer cells. It suggests that ZON is involved in the modulation of ferroptosis in cervical cancer progression.

Furthermore, regarding the mechanism, we identified that ZON enhanced miR-506-3p expression and CD164 was a target of miR-506-3p, in which ZON inhibited CD164

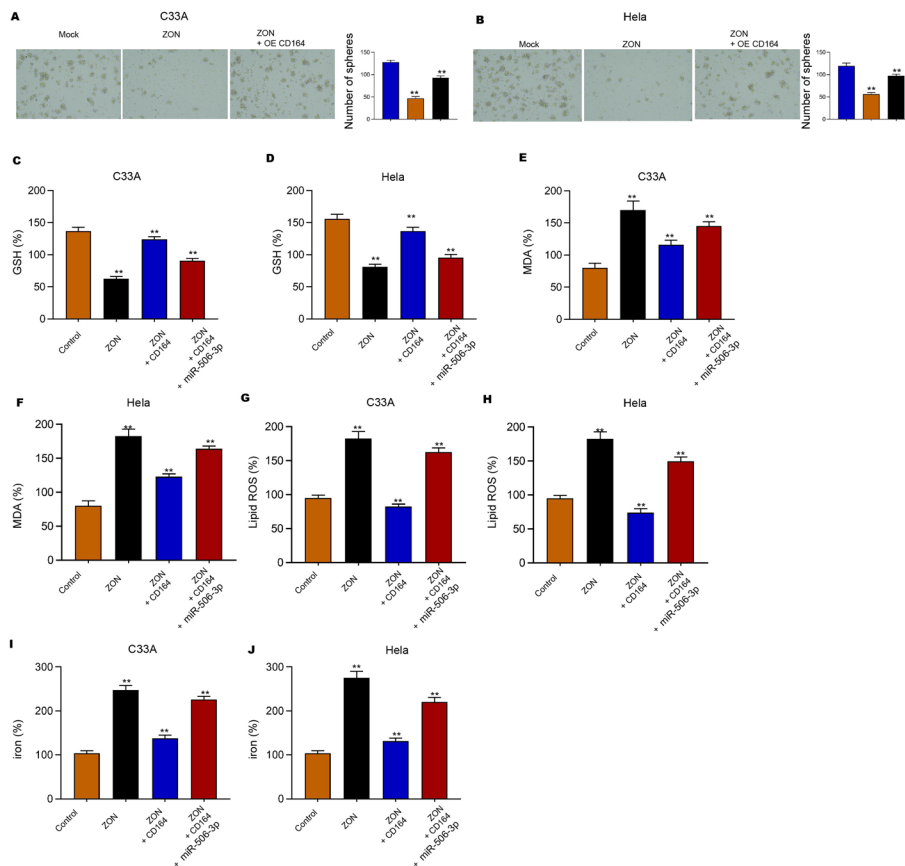


Fig. 7 ZON represses stemness and reduces ferroptosis of cervical cancer cells by targeting CD164. **A, B** Sphere formation efficiency was detected by sphere formation assays. **C–J** Levels of GSH (**C, D**), MDA (**E, F**), lipid ROS (**G, H**), and iron (**I, J**) were analyzed. The experiments were repeated 3 times, ** $P < 0.01$

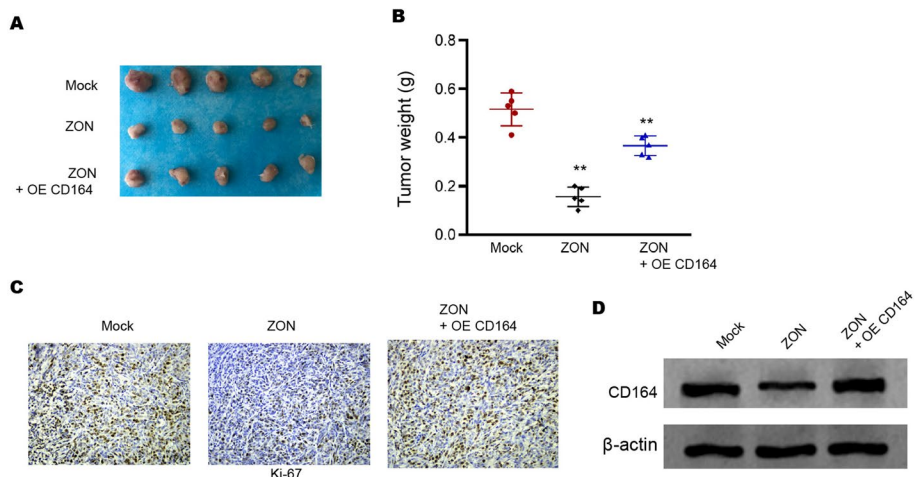


Fig. 8 ZON inhibits cell growth of cervical cancer in vivo by targeting CD164. **A–D** Tumor growth of C33A cell was analyzed by xenograft mouse model in vivo ($n = 5$). The tumor images (**A**), tumor weight (**B**), Ki-67 levels (**C**), and CD164 expression (**D**) were shown. The experiments were repeated 3 times, ** $P < 0.01$

expression by promoting miR-506-3p in cervical cancer cells. We validated that CD164 reversed miR-506-3p-mediated stemness and ferroptosis in cervical cancer cells. ZON repressed stemness and reduced ferroptosis of cervical cancer cells by targeting CD164. ZON inhibits cell growth of cervical cancer *in vivo* by targeting CD164. It has been reported that miR-506-3p inhibits tumorigenesis by modulating YAP1 in thyroid cancer (Chen et al. 2020). MiR-506-3p represses ovarian cancer progression by negatively modulating MTMR6 expression (Wang et al. 2019). Exosomal circPACRGL contributes to colorectal cancer development by miR-142-3p/miR-506-3p/TGF- β 1 axis (Shang et al. 2020). CD164 contributes to the progression of bladder cancer and is correlated with a poor prognosis (Zhang et al. 2018). MiR-219a-5p modulates the radiotherapy sensitivity by targeting CD164 in non-small cell lung cancer cells (Wei et al. 2020). CD164 is involved in the regulation of tumorigenesis by SDF-1 α /CXCR4 signaling in ovarian surface epithelial cells (Huang et al. 2013). However, the function of miR-506-3p and CD164 in stemness and reduced ferroptosis of cervical cancer cells is unreported. We discovered the potential mechanism involving miR-506-3p and CD164 of circFoxo3-mediated cervical cancer phenotypes. A more detailed relationship between miR-506-3p, CD164, and circFoxo3 should be verified *in vitro* and *in vivo*, and at clinical levels. Other potential downstream factors of circFoxo3 and miR-506-3p need to confirm in future experiments.

There are still some limitations and unresolved scientific problems in the current study. It has been reported the anti-cancer effect of ZON in many previous reports and we identified that ZON regulated the ferroptosis, proliferation, invasion and stemness of cervical cancer by miR-506-3p/CD164 signaling. However, why Zinc oxide targets cervical cancer cells in particular compared to normal cells and how it affects miR-506-3p/CD164 regulatory axis are still unclear, which need to be explored in future investigations by more detailed studies.

Conclusions

In brief, we concluded that ZON regulated the ferroptosis, proliferation, invasion and stemness of cervical cancer by miR-506-3p/CD164 signaling. ZON may become a promising therapeutic approach for cervical cancer.

Abbreviations

CSC	Cancer stem cell
ZON	Zinc oxide nanoparticle
TGF- β 1	Transforming growth factor- β 1

Supplementary Information

The online version contains supplementary material available at <https://doi.org/10.1186/s12645-022-00134-x>.

Additional file 1: Figure S1 Characterization of ZON. **A, B** ZON was synthesized and the actual size and surface charge were observed by TEM and zeta potential analyzer. **Figure S2** Effect of ZON on HcerEpic cells. **A** HcerEpic cells were treated with ZON. The cell growth was analyzed by colony formation assays. *Ns* no significant. **Figure S3** ZON inhibits cell growth of cervical cancer *in vivo* by targeting CD164. **A–D** Tumor growth of Hela cell was analyzed by xenograft mouse model *in vivo* ($n=5$). The tumor images (**A**), tumor weight (**B**), Ki-67 levels (**C**), and CD164 expression (**D**) were shown. The experiments were repeated 3 times, ** $P < 0.01$.

Acknowledgements

Not applicable.

Author contributions

HL and JL designed the study; YL performed experiments; SL collected and analyzed data; FL wrote the manuscript; All authors read and approved the final manuscript.

Funding

Not applicable.

Availability of data and materials

The data sets used and/or analysed during the current study are available from the corresponding author on reasonable request.

Declarations**Ethics approval and consent to participate**

Not applicable.

Consent for publication

Not applicable.

Competing interests

The authors declare that they have no conflict of interest.

Received: 13 December 2021 Accepted: 13 September 2022

Published online: 22 October 2022

References

- Alvarez SW, Sviderskiy VO, Terzi EM, Papagiannakopoulos T, Moreira AL, Adams S et al (2017) NFS1 undergoes positive selection in lung tumours and protects cells from ferroptosis. *Nature* 551:639–643
- Anitha J, Selvakumar R, Murugan K (2019) Chitosan capped ZnO nanoparticles with cell specific apoptosis induction through P53 activation and G2/M arrest in breast cancer cells—In vitro approaches. *Int J Biol Macromol* 136:686–696
- Bae GU, Gaio U, Yang YJ, Lee HJ, Kang JS, Krauss RS (2008) Regulation of myoblast motility and fusion by the CXCR4-associated sialomucin, CD164. *J Biol Chem* 283:8301–8309
- Bhatla N, Singhal S (2020) Primary HPV screening for cervical cancer. *Best Pract Res Clin Obstet Gynaecol* 65:98–108
- Chen L, Wang X, Ji C, Hu J, Fang L (2020) MiR-506-3p suppresses papillary thyroid cancer cells tumorigenesis by targeting YAP1. *Pathol Res Pract* 216:153231
- Cohen PA, Jhingran A, Oaknin A, Denny L (2019) Cervical cancer. *Lancet* 393:169–182
- Doyonnas R, Yi-Hsin Chan J, Butler LH, Rappold I, Lee-Prudhoe JE, Zannettino AC et al (2000) CD164 monoclonal antibodies that block hemopoietic progenitor cell adhesion and proliferation interact with the first mucin domain of the CD164 receptor. *J Immunol* 165:840–851
- Forde S, Tye BJ, Newey SE, Roubelakis M, Smythe J, McGuckin CP et al (2007) Endolyn (CD164) modulates the CXCL12-mediated migration of umbilical cord blood CD133+ cells. *Blood* 109:1825–1833
- Havens AM, Jung Y, Sun YX, Wang J, Shah RB, Buhning HJ et al (2006) The role of sialomucin CD164 (MGC-24v or endolyn) in prostate cancer metastasis. *BMC Cancer* 6:195
- Hu C, Du W (2020) Zinc oxide nanoparticles (ZnO NPs) combined with cisplatin and gemcitabine inhibits tumor activity of NSCLC cells. *Aging (alban NY)* 12:25767–25777
- Hu Z, Mi Y, Qian H, Guo N, Yan A, Zhang Y et al (2020) A potential mechanism of temozolomide resistance in glioma-ferroptosis. *Front Oncol* 10:897
- Huang AF, Chen MW, Huang SM, Kao CL, Lai HC, Chan JY (2013) CD164 regulates the tumorigenesis of ovarian surface epithelial cells through the SDF-1alpha/CXCR4 axis. *Mol Cancer* 12:115
- Liu HJ, Hu HM, Li GZ, Zhang Y, Wu F, Liu X et al (2020) Ferroptosis-related gene signature predicts glioma cell death and glioma patient progression. *Front Cell Dev Biol* 8:538
- Lytle NK, Barber AG, Reya T (2018) Stem cell fate in cancer growth, progression and therapy resistance. *Nat Rev Cancer* 18:669–680
- Mou Y, Wang J, Wu J, He D, Zhang C, Duan C et al (2019) Ferroptosis, a new form of cell death: opportunities and challenges in cancer. *J Hematol Oncol* 12:34
- Nabil A, Elshemy MM, Asem M, Abdel-Motaal M, Gomaa HF, Zahran F et al (2020) Zinc oxide nanoparticle synergizes sorafenib anticancer efficacy with minimizing its cytotoxicity. *Oxid Med Cell Longev* 2020:1362104
- Ruenraroengsak P, Kiryushko D, Theodorou IG, Klosowski MM, Taylor ER, Niriella T et al (2019) Frizzled-7-targeted delivery of zinc oxide nanoparticles to drug-resistant breast cancer cells. *Nanoscale* 11:12858–12870
- Shang A, Gu C, Wang W, Wang X, Sun J, Zeng B et al (2020) Exosomal circPACRGL promotes progression of colorectal cancer via the miR-142-3p/miR-506-3p- TGF-beta1 axis. *Mol Cancer* 19:117
- Song H, Nan Y, Wang X, Zhang G, Zong S, Kong X (2017) MicroRNA613 inhibits proliferation and invasion of renal cell carcinoma cells through targeting FZD7. *Mol Med Rep* 16:4279–4286
- Steele A, Bayer I, Loth E (2009) Inherently superoleophobic nanocomposite coatings by spray atomization. *Nano Lett* 9:501–505
- Tang J, Zhang L, She X, Zhou G, Yu F, Xiang J et al (2012) Inhibiting CD164 expression in colon cancer cell line HCT116 leads to reduced cancer cell proliferation, mobility, and metastasis in vitro and in vivo. *Cancer Invest* 30:380–389
- The L (2020) Eliminating cervical cancer. *Lancet* 395:312

- Vu M, Yu J, Awolude OA, Chuang L (2018) Cervical cancer worldwide. *Curr Probl Cancer* 42:457–465
- Wahab R, Siddiqui MA, Saquib Q, Dwivedi S, Ahmad J, Musarrat J et al (2014) ZnO nanoparticles induced oxidative stress and apoptosis in HepG2 and MCF-7 cancer cells and their antibacterial activity. *Colloids Surf B Biointerfaces* 117:267–276
- Wang Y, Lei X, Gao C, Xue Y, Li X, Wang H et al (2019) MIR-506–3p suppresses the proliferation of ovarian cancer cells by negatively regulating the expression of MTMR6. *J Biosci*. <https://doi.org/10.1007/s12038-019-9952-9>
- Wang Y, Zhao G, Condello S, Huang H, Cardenas H, Tanner EJ et al (2021) Frizzled-7 identifies platinum-tolerant ovarian cancer cells susceptible to ferroptosis. *Cancer Res* 81:384–399
- Wei T, Cheng S, Fu XN, Feng LJ (2020) miR-219a-5p enhances the radiosensitivity of non-small cell lung cancer cells through targeting CD164. *Biosci Rep*. <https://doi.org/10.1042/BSR20192795>
- Yagoda N, von Rechenberg M, Zaganjor E, Bauer AJ, Yang WS, Fridman DJ et al (2007) RAS-RAF-MEK-dependent oxidative cell death involving voltage-dependent anion channels. *Nature* 447:864–868
- Zhang XG, Zhang T, Li CY, Zhang MH, Chen FM (2018) CD164 promotes tumor progression and predicts the poor prognosis of bladder cancer. *Cancer Med* 7:3763–3772
- Zhou LY, Zhai M, Huang Y, Xu S, An T, Wang YH et al (2019) The circular RNA ACR attenuates myocardial ischemia/reperfusion injury by suppressing autophagy via modulation of the Pink1/FAM65B pathway. *Cell Death Differ* 26:1299–1315

Publisher's Note

Springer Nature remains neutral with regard to jurisdictional claims in published maps and institutional affiliations.

Ready to submit your research? Choose BMC and benefit from:

- fast, convenient online submission
- thorough peer review by experienced researchers in your field
- rapid publication on acceptance
- support for research data, including large and complex data types
- gold Open Access which fosters wider collaboration and increased citations
- maximum visibility for your research: over 100M website views per year

At BMC, research is always in progress.

Learn more biomedcentral.com/submissions

